

SYNTHETIC DATA DESCRIPTION

Data generated using Simcenter Prescan

Abstract

The synthetic data structure and data content is described in the document

Alexandru Forrai Ph.D.
alexandru.forrai@siemens.com



This work has received funding from the European Union's Horizon Europe research and innovation program under grant agreement No 101076754 - Althena project.

Contents

1 Ground truth data format – brief description	2
2. Physics-based camera sensor data	4
3. Point cloud and physics-based LiDAR sensor data.....	5
4. Physics-based radar sensor data.....	8
4.1 Radar Scene Simulator	10
5. Depth camera	13
6. Synthetic data generation considering variations of VRUs, weather and illumination	14
7. Synthetic data folder structure.....	16
8. References.....	17

1 Ground truth data format – brief description

The ground truth data format basically extends the well-known KITTI data format [1,2] with unique ObjectID as well as object type according to Simcenter Prescan [3] (see Table 1.1).

Table 1.1: Data structure – Simcenter Prescan ground truth

Values	Name	Description
1	object ID	Unique object ID from Prescan
1	object type	Describes the type of the object based on Simcenter Prescan object types

#Values	Name	Description
1	type	Describes the type of object: 'Car', 'Van', 'Truck', 'Pedestrian', 'Person_sitting', 'Cyclist', 'Tram', 'Misc' or 'DontCare'
1	truncated	Float from 0 (non-truncated) to 1 (truncated), where truncated refers to the object leaving image boundaries
1	occluded	Integer (0,1,2,3) indicating occlusion state: 0 = fully visible, 1 = partly occluded 2 = largely occluded, 3 = unknown
1	alpha	Observation angle of object, ranging [-pi..pi]
4	bbox	2D bounding box of object in the image (0-based index): contains left, top, right, bottom pixel coordinates
3	dimensions	3D object dimensions: height, width, length (in meters)
3	location	3D object location x,y,z in camera coordinates (in meters)
1	rotation_y	Rotation ry around Y-axis in camera coordinates [-pi..pi]
1	score	Only for results: Float, indicating confidence in detection, needed for p/r curves, higher is better.

As a remark, occlusion of the objects is calculated only considering the 2D projections of the objects (the height of the object is neglected). When the objects enter or exit the field of view of the sensor, the occlusion value might flicker. Furthermore, for small objects, which are far away a similar effect might happen since the number of imaginary rays intersecting the object might be very low.

Currently, in the field of view of the ground-truth sensor 100 imaginary rays are considered, based on which the occlusion is calculated. A higher number of imaginary rays could improve the precision of occlusion calculations but will increase the computational effort.

All distances are relative to the ground truth sensor, which is placed in the same position as the physics-based camera. The observation angle as well as the rotation angle are shown in the Fig. 1.1.

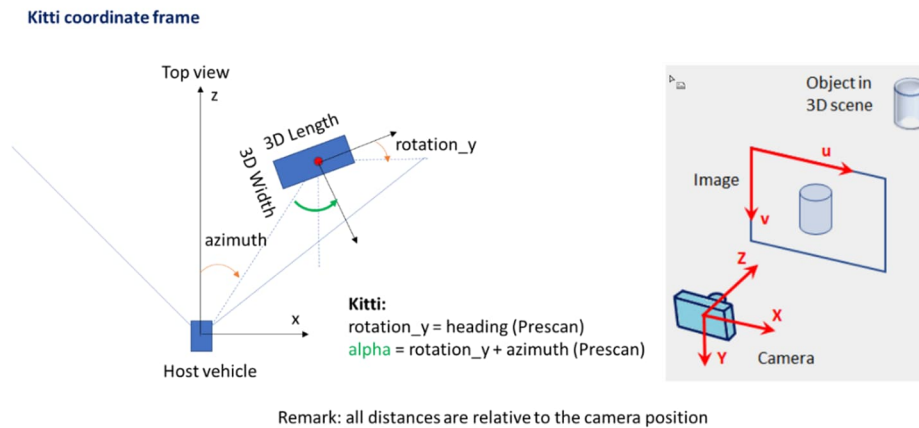


Fig. 1.1 Ground truth data and coordinate frames

Remarks: the direction of the arrow shows from which line to which line the angle is measured. The arrow direction does contain information about the sign of the angle as follows:

- If the angle is measured CCW then is positive
- If the angle is measured CW then is negative

In this way the angle is in the $[-\pi, \pi]$ interval.

Information about the host vehicle is stored into a “prescanParameters.json” file, see Fig. 1.2. The relative position of all sensors are defined in the vehicle coordinate frame. In Simcenter Prescan the relative position of the sensors is defined against the rear axle center (see screenshots in this document). In case of the synthetic data, the relative position of the sensors is defined against the center of the bounding box (see “prescanParameters.json” file). These relative positions are illustrated in Fig. 1.3.

```

Ego:
  bboxSize3D:
    length: 3.950000047683716
    width: 1.9700000286102295
    height: 1.4500000476837158
  KittiTypeName: "Car"
  KittiTypeId: 1
  PrescanTypeName: "Car"
  PrescanTypeId: 1
  Ego: true
  Sensor: {...}
    
```

Fig. 1.2 Information about the host vehicle stored in .json file format

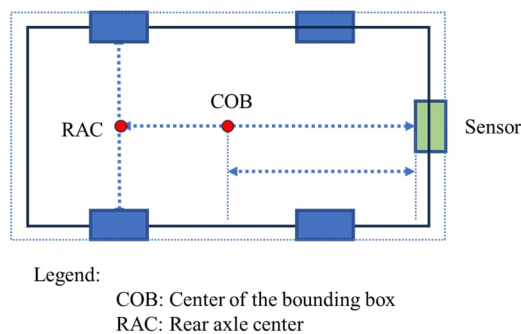


Fig. 1.3 Relative position of the sensor in vehicle coordinate frame

2. Physics-based camera sensor data

The physics-based camera position is defined relative to the center of the host vehicle bounding box center (see Fig. 2.1). Information about camera position and camera parameters as well as the camera intrinsic matrix are stored into a “prescanParameters.json” file.

The camera data saved in .jpeg format, the images are concatenated and saved into an .mp4 video file.

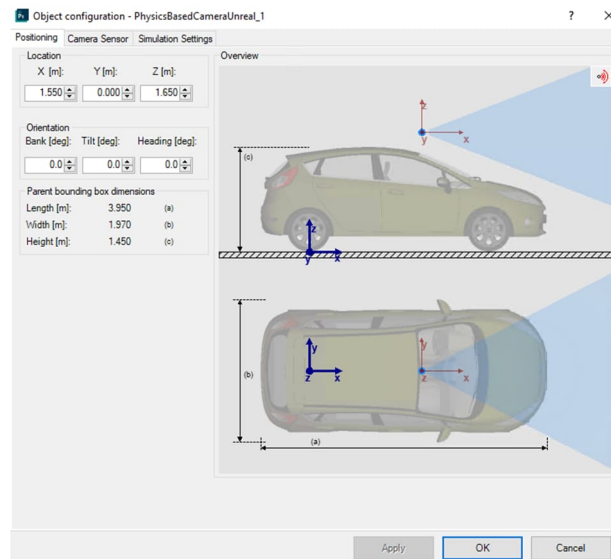


Fig. 2.1 Physics-based camera position

The physics-based camera sensor in Simcenter Prescan is a virtual model of the real camera, mentioned below [4, 5]:

- Model: a2A1920-51gcPRO Basler ace 2 GigE camera
- Size (L * W * H) / Weight: 62.2 * 29 * 29 mm / < 105 g
- Resolution (H x V Pixels): 1920 x 1200
- Pixel Size (H x V): 3.45 μm x 3.45 μm
- Frame Rate: 24 (depending on light conditions – exposure time)
- Field of view:
 - Vertical: 54.3°
 - Horizontal: 79°
- Len: C125-0418-5M-P f4mm

3. Point cloud and physics-based LiDAR sensor data

The point cloud ideal LiDAR sensor settings are described below.

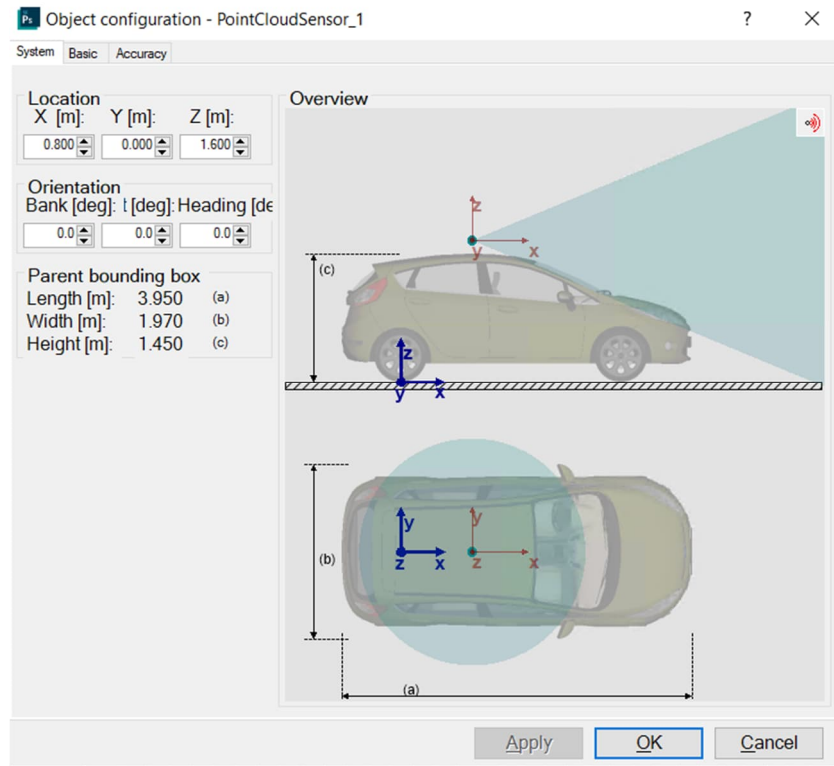


Fig. 3.1 Point cloud ideal LiDAR sensor settings

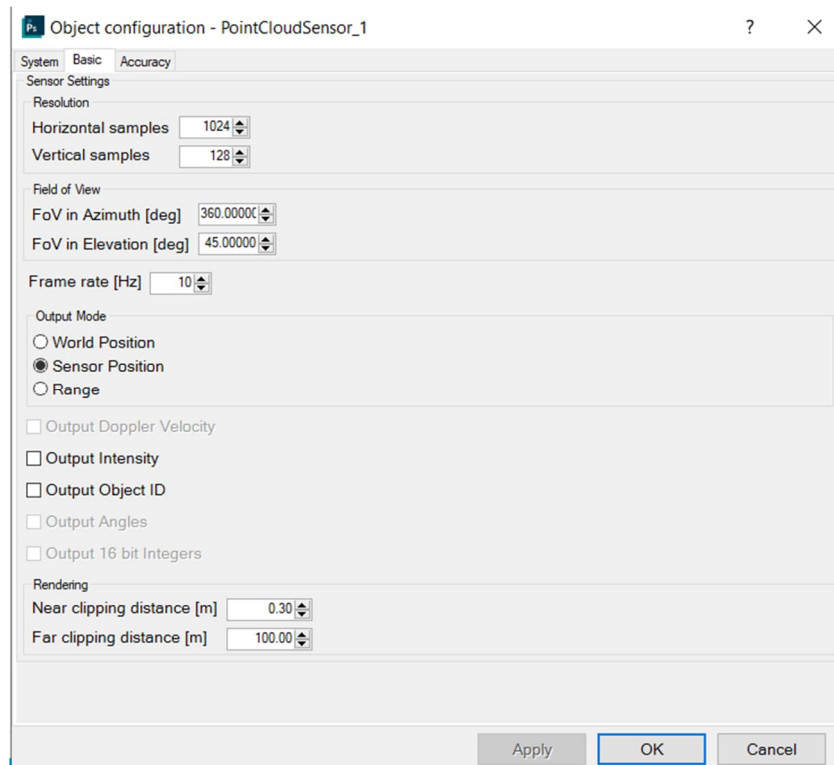


Fig. 3.2 Point cloud ideal LiDAR sensor settings

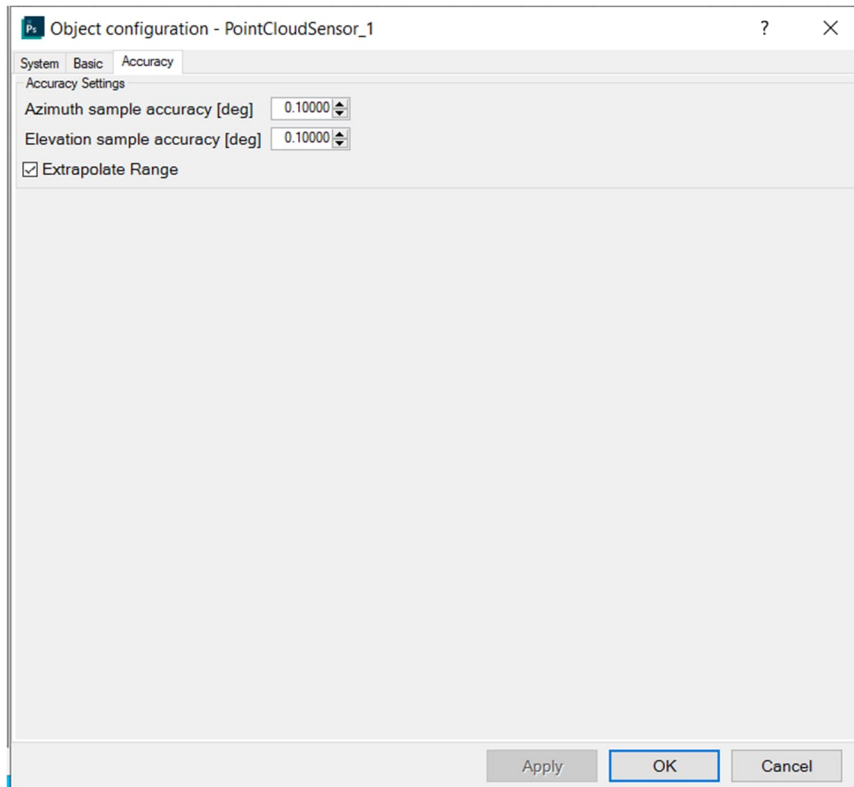


Fig. 3.3 Point cloud ideal LiDAR sensor settings

The physics-based LiDAR sensor settings are described below.

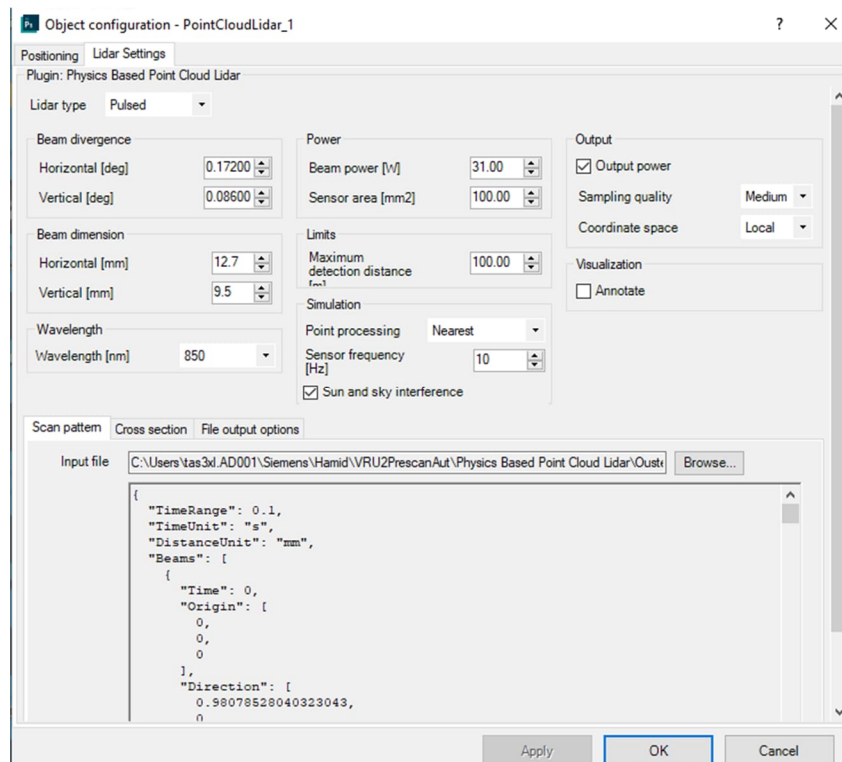


Fig. 3.4 Physics-based LiDAR sensor settings

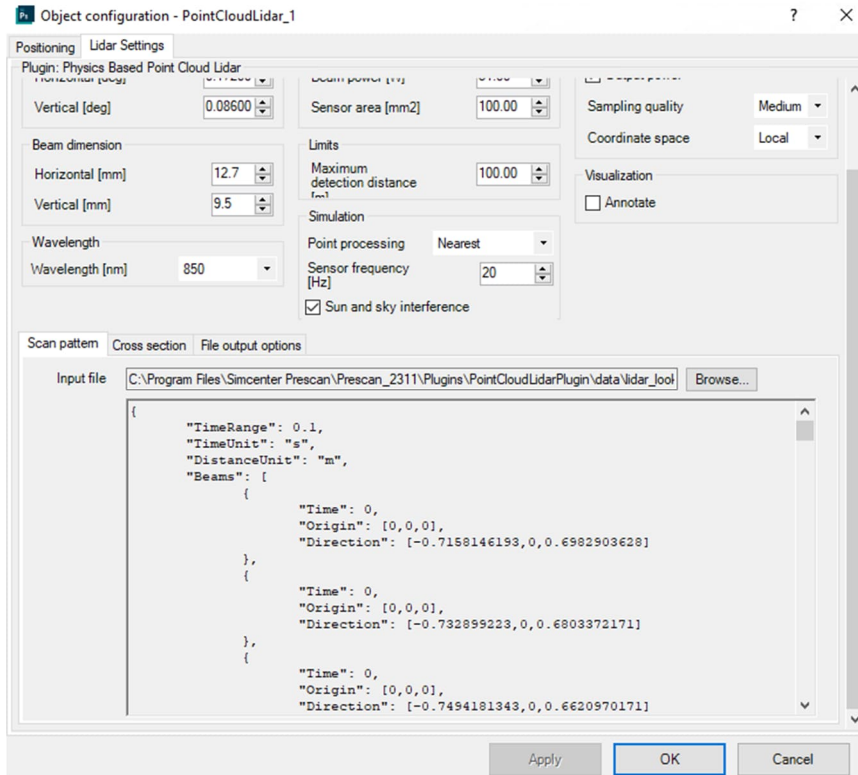


Fig. 3.5 Physics-based LiDAR sensor settings

The physics-based LiDAR sensor in Simcenter Prescan is a virtual model of the real LiDAR sensor, mentioned below [6]:

Model: Ouster OS2-128

- Dimensions:
 - Diameter: 119.6 mm (4.71 in)
 - Height: 98.9 mm (3.89 in)
- Weight: 1100 g
- Vertical Resolution: 128 channels
- Horizontal Resolution: 1024
- Field of View:
 - Vertical: 22.5° (+11.25° to -11.25°)
 - Horizontal: 360°
- Range:
 - Minimum 1 m
 - Maximum: 240 m
- Range Resolution: 0.1 cm
- Rotation Rate: 10 Hz
- Laser Wavelength: 865 nm
- Points Per Second: 2,621,440 (128 channel)
- Data Per Point: Range, signal, reflectivity, near-infrared, channel, azimuth angle, timestamp
- Timestamp Resolution: < 1 μs
- Data Latency: < 10 ms

4. Physics-based radar sensor data

The radar data processing pipeline is illustrated in Fig. 4.1, where after the analog-to-digital conversion (ADC) fast Fourier transforms, and user specific processing takes place. These last two steps currently are not part of Simcenter Prescan and can be done by the user.

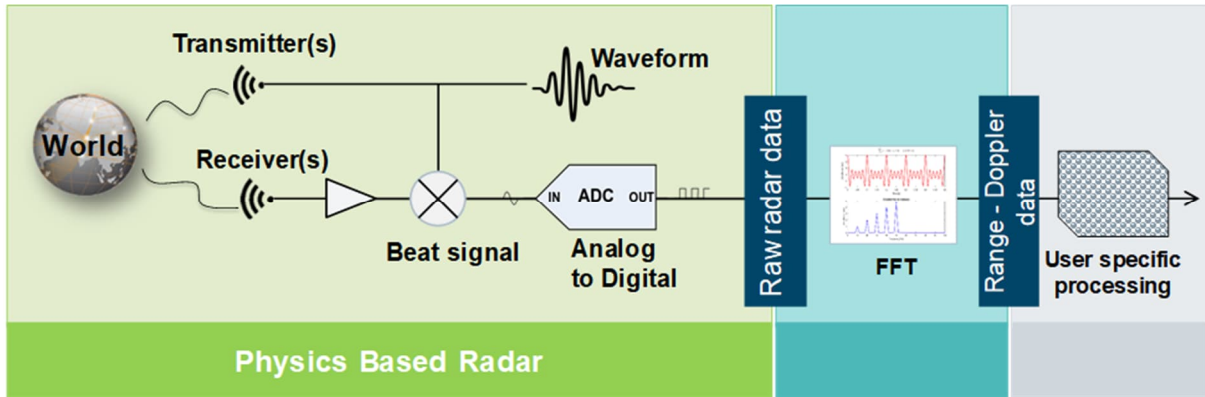


Fig. 4.1 Radar data processing pipeline

For a better understanding of the operation principle of the radar sensor, the basic notions: transmitter, receiver, chirps and samples are illustrated in Fig. 4.2 [7,8].

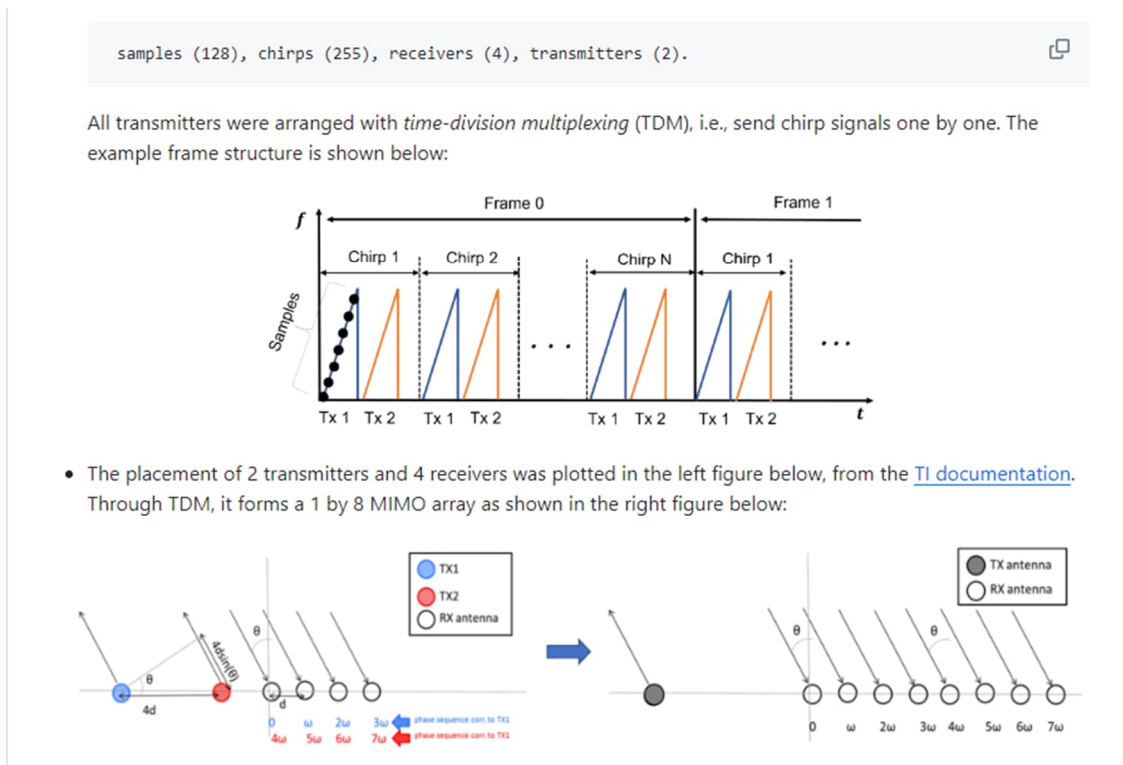


Fig. 4.2 Possible arrangements of transmitters, receivers, chirps and samples

The settings of the physics-based radar in Simcenter Prescan are illustrated in Fig. 4.3 and Fig. 4.4.

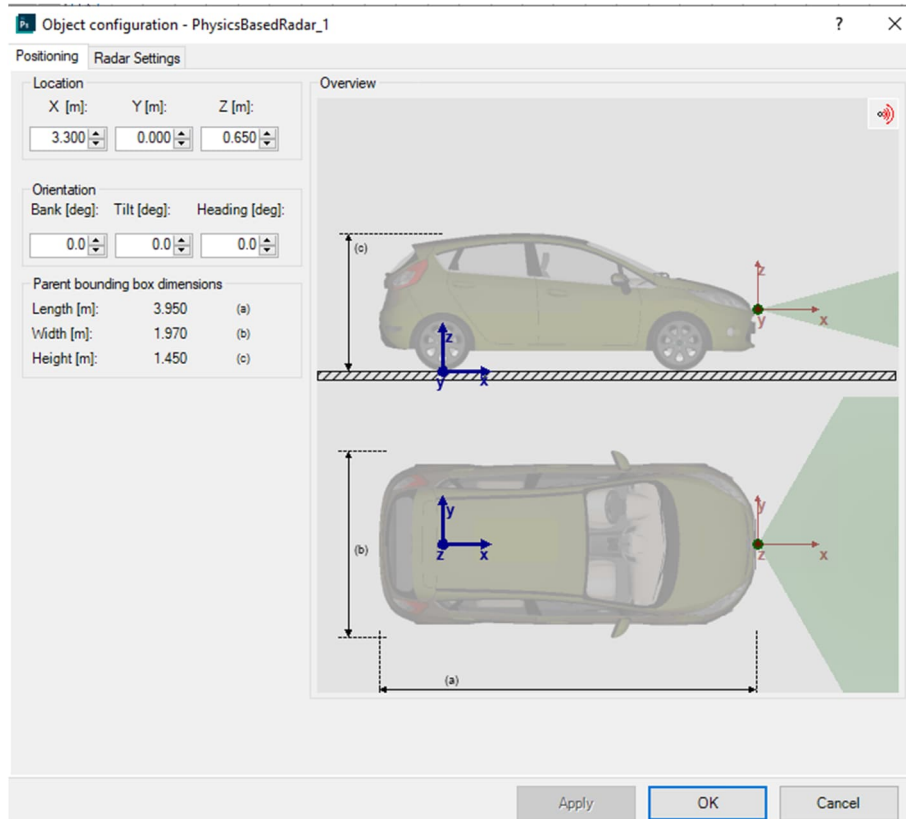


Fig. 4.3 Physics-based radar sensor settings

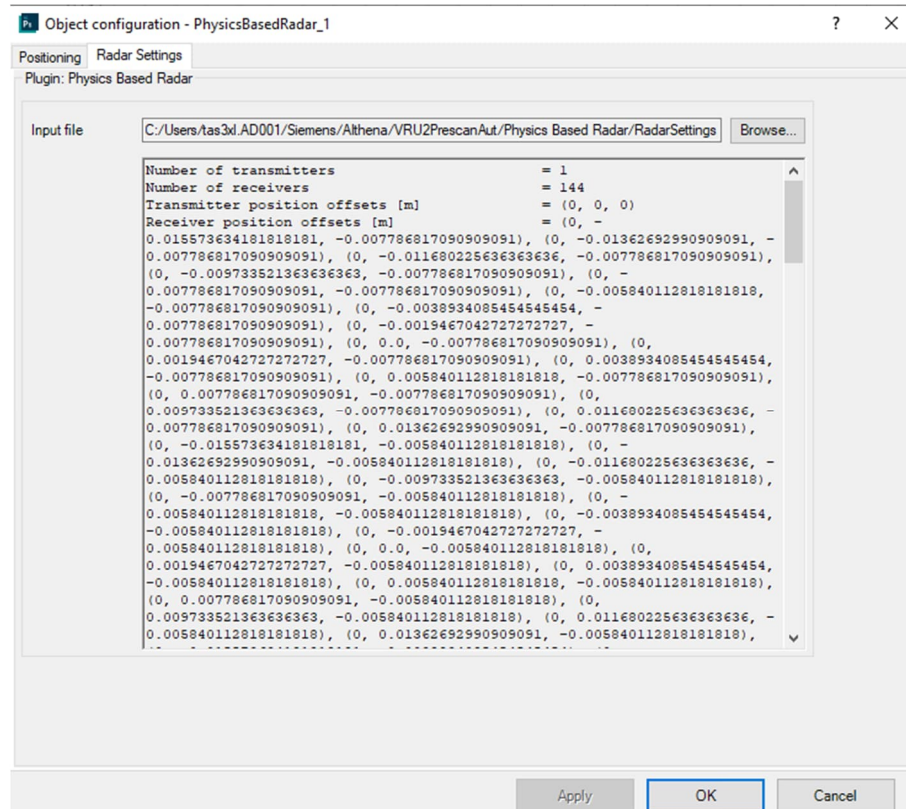


Fig. 4.4 Physics-based radar sensor settings

The radar detections are illustrated in Fig. 4.5 and are stored for each timestamp in a .txt file having the following structure, see Table 4.1.

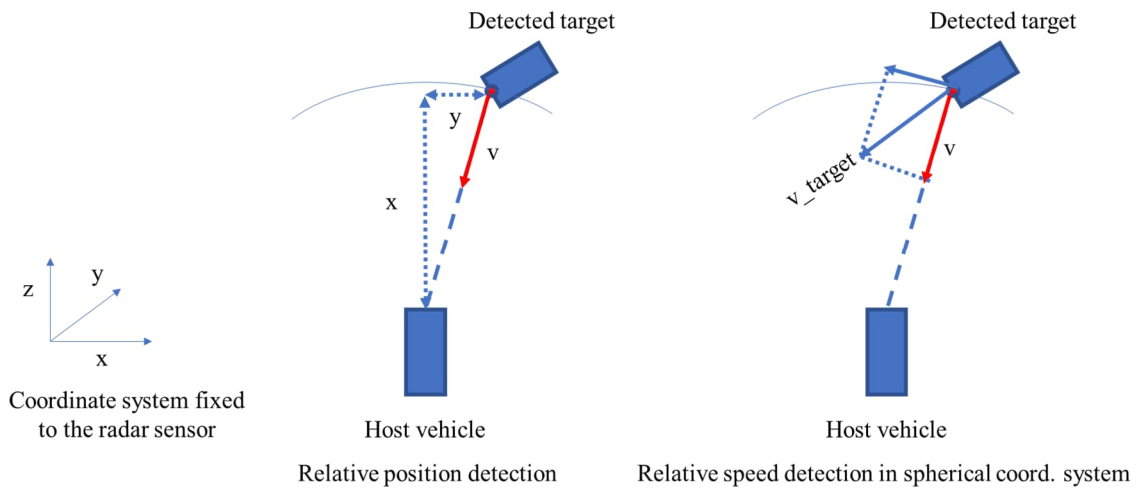


Fig. 4.5 Physics-based radar sensor detection – position and speed

Table 4.1: Radar detections – data structure

Radar detections	Longitudinal distance x [m]	Lateral distance y [m]	Elevation z [m]	Relative velocity in spherical coordinate system [m/s]	Power of the reflected radar signal for that detection [dB]
Object 1					
...					
Object n					

Since the generated ADC output leads to extremely large files a new feature of Simcenter Prescan has been used, which is called “Radar Scene Simulator”.

4.1 Radar Scene Simulator

The “Radar Scene Simulator” in a strict sense is not a physics-based radar sensor model, one of the main differences is that the signal to noise ratio is not considered. Therefore, the detections are kind of ideal detections, so the user should add signal to noise model according to the measurements.

The output of the radar scene simulator is saved in .pcd format.

Material Assignment

When adding objects to the experiment, radar materials are automatically assigned according to the following substitutions (see Table 4.2):

Table 4.2: Material assignments in Simcenter Prescan

Material	Radar Material
Plastic	Asphalt
Asphalt, (wet, dark, light, etc.)	Asphalt
Grass (dark, light)	Grass

Fabrics (cotton wool, leather, etc.)	Perfect conductor ¹
Reflective sheet, Reflector	Perfect conductor
Skin	Perfect conductor ¹
Car paint	Perfect conductor
Road modifiers (Road markers, dirt spots, road cracks, etc.)	Transparent ²
Traffic sign Pole	Perfect conductor
Cement guardrail, sound absorbing wall	Smooth asphalt
Chain fence	Transparent ²
Information board	Asphalt
Embankments	Grass
Transparent	Transparent
Fully Absorbent	Fully Absorbent
Default	Asphalt

¹ Fabrics and skin use the perfect conductor radar material as it closely approximates the radar signature of a real person.

² Not supported by the Radar Scene Simulator.

The radar scene simulator sensor position and the basic settings are shown in Fig. 4.5 and Fig. 4.6.

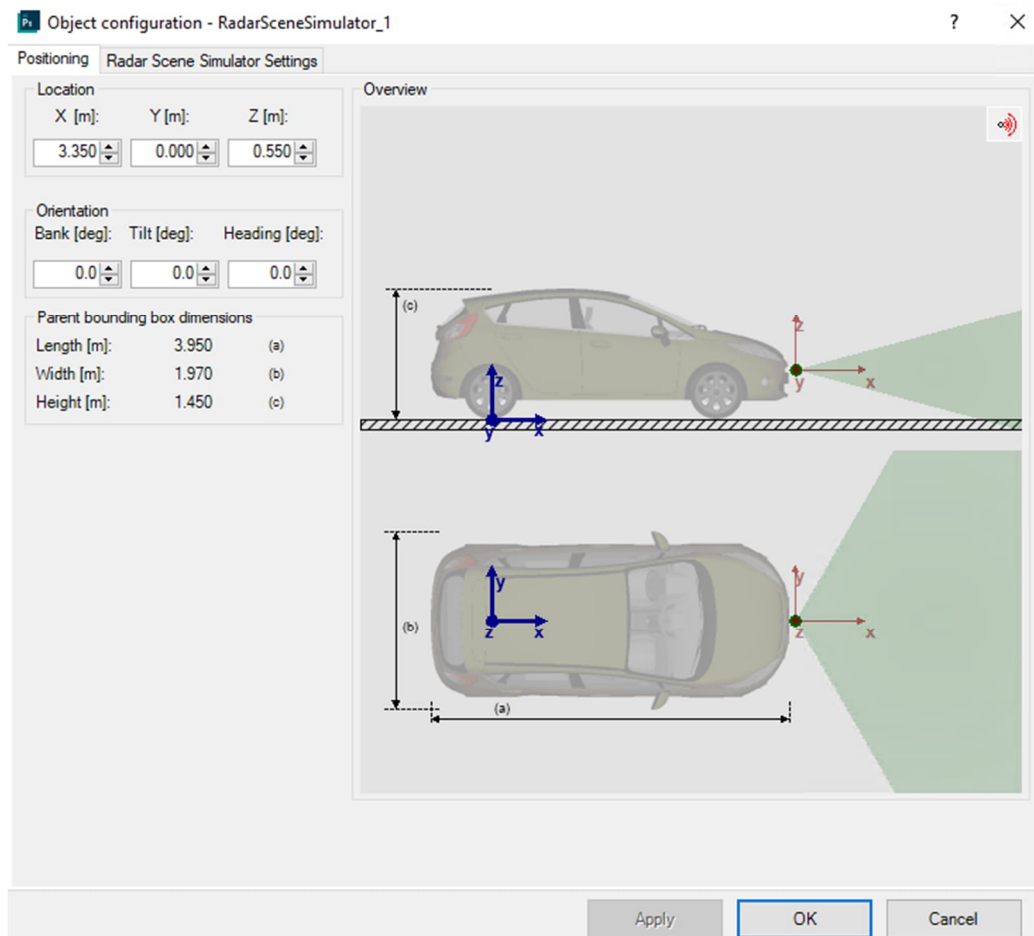


Fig. 4.5 Radar sensor position in case of radar scene simulator

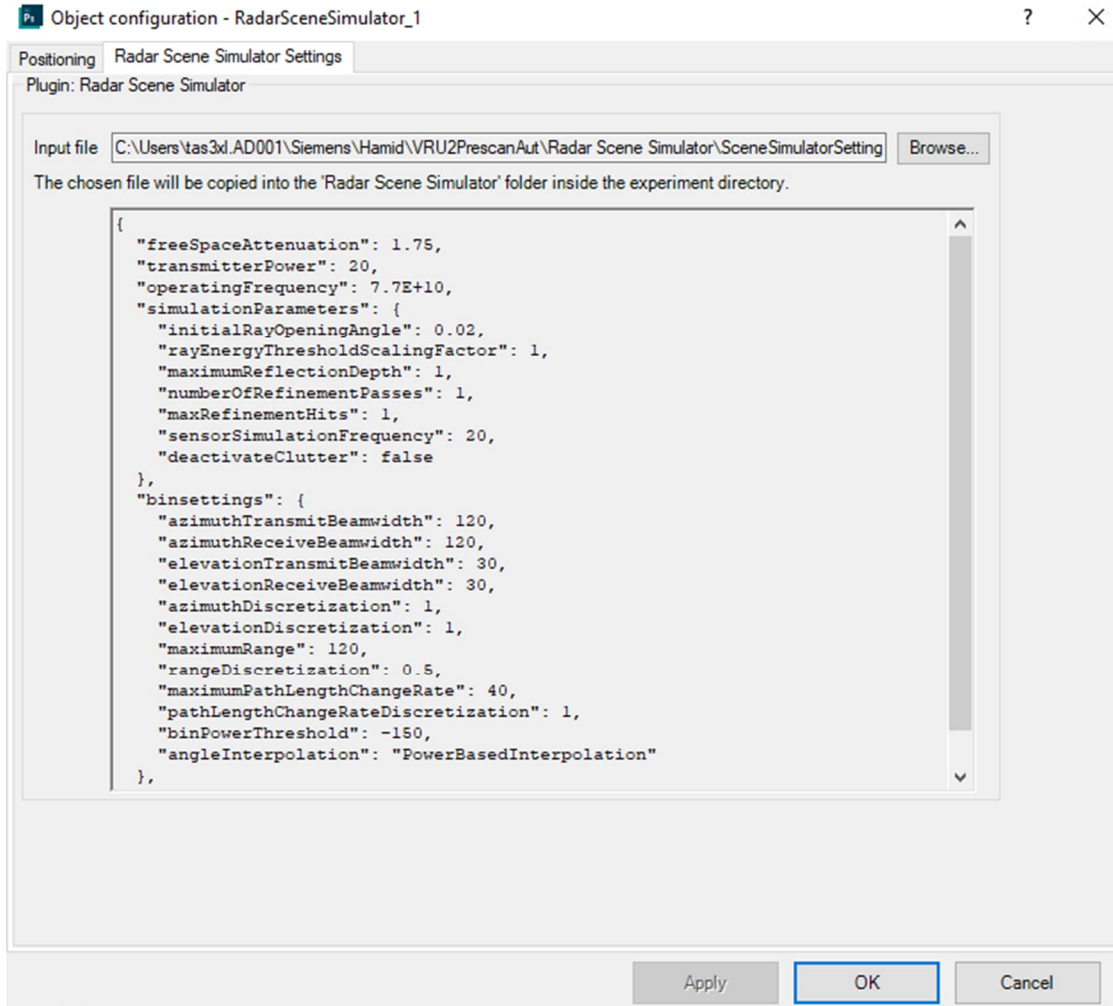


Fig. 4.6 Radar sensor settings in case of radar scene simulator

The attenuation factors considering different weather conditions are mentioned in Table. 4.3 [9-11]. In the synthetic data set the radar scene simulator data is included and saved as .pcd files.

Table 4.3: Attenuation factors function on weather conditions

Weather	'Clear'	Rain'	'Light Fog'	'Dense Fog'	'Snow and Light Fog'
Attenuation factor [dB]	0.3470	4.5	1.5	1.75	1.6

5. Depth camera

The depth camera provides a 'camera' image with depth values instead of colors. It provides ground truth data which can be used i.e. to calibrate or validate camera depth calculations. The depth camera sensor settings are shown below Fig. 5.1 and Fig. 5.2.

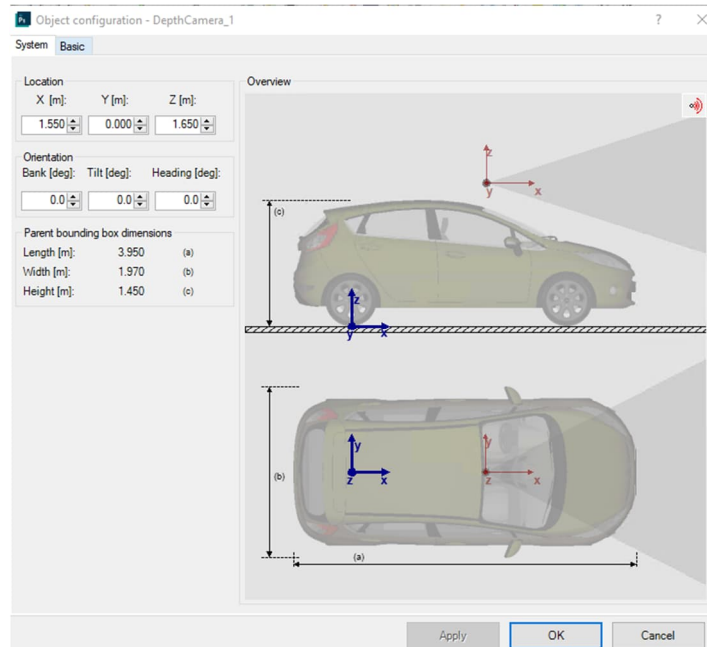


Fig. 5.1 Depth camera settings – camera position and orientation

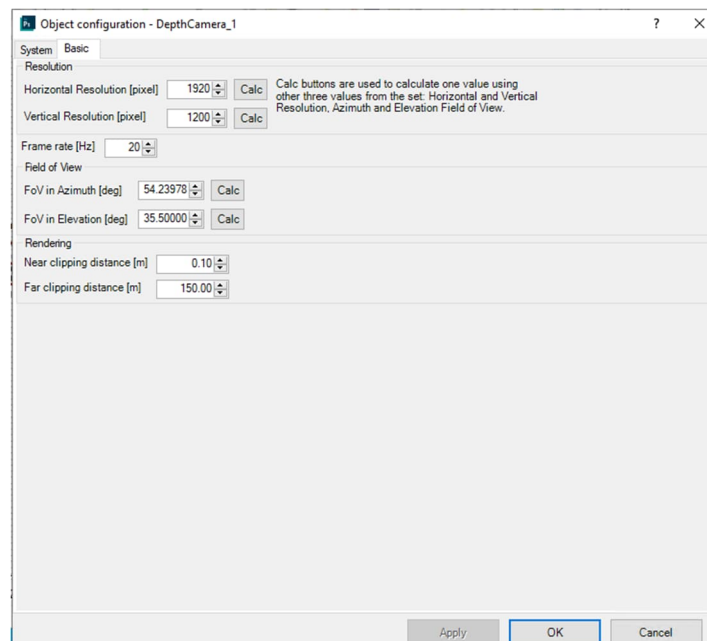


Fig. 5.2 Depth camera settings – camera configuration

Based on the near and far clipping distance and the images provided, the absolute depth can be calculated.

6. Synthetic data generation considering variations of VRUs, weather and illumination

During the synthetic data generation, it is assumed that the operational design domain is Amsterdam city, The Netherlands.

The sun position defined by azimuth and elevation, depends on the season as well as time during the day, as shown in Fig. 6.1 and Fig. 6.2 [12].

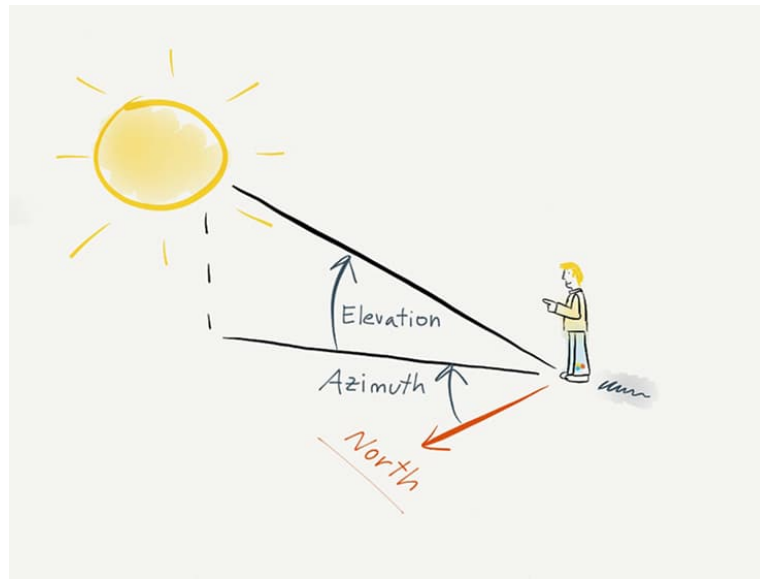


Fig. 6.1 Sun position defined by azimuth and elevation

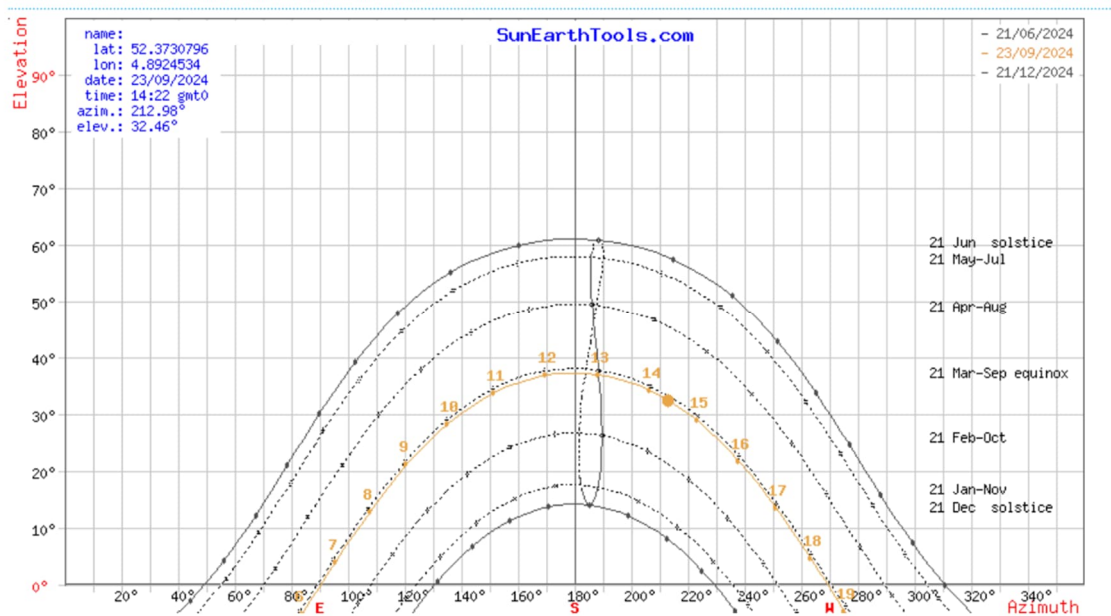


Fig. 6.2 Sun position in Amsterdam during the year at different moments of the day [12]

In the aim to keep things simple, we considered only five different time moments during the day, and we have three distinctive seasons from sun position perspective: spring or autumn, summer and winter. These are summarized in Table 6.1.

Table 6.1: Considered sun positions: season and time.

Spring or Autumn					
Time [hour]	07	10	12:30	17	18
Azimuth [deg]	95	140	180	220	265
Elevation [deg]	7	30	38	30	9
Summer					
Time [hour]	06:30	10	12:30	16	20
Azimuth [deg]	60	117	180	250	300
Elevation [deg]	8	48	60	45	8
Winter					
Time [hour]	08:30	10	12:30	15	17:30
Azimuth [deg]	120	145	180	210	220
Elevation [deg]	0	7	15	9	0

In terms of vulnerable road users, we considered only 5 different categories as mentioned below:

$$F1 = \{Person, Person_wBuggy, Person_Cycling, Person_wCart, Child_Regular\}$$

In terms of time moments during the day we considered 5 different time moments, as specified in Table 6.1.

$$F2 = \{Time_1, Time_2, Time_3, Time_4, Time_5\}$$

In terms of weather, based on the season we defined per season maximum 4 different weather types, as shown in Table 6.2.

Table 6.2: Weather types, function of season

Spring or Autumn				
Weather	Clear	Rain	Light_Fog	Dense_Fog
Summer				
Weather	Clear	Rain		
Winter				
Weather	Clear	Rain	Snow	Snow_and_Light_Fog

$$F3 = \{Weather_1, Weather_2, Weather_3, Weather_4\}$$

In terms of seasons, we have three distinctive seasons from illumination point of view:

$$F4 = \{Spring_or_Autumn, Summer, Winter\}$$

We remark that the data set is generated using a combinatorial testing approach. Combinatorial or t-way testing is a proven method for more effective testing at lower cost. Studies by NIST research showed that most software bugs and failures are caused by one or two parameters, with progressively fewer by three or more, which means that combinatorial testing can provide more efficient fault detection than conventional methods. New algorithms compressing combinations into a small number of tests have made this method practical for industrial use, providing better testing at lower cost.

Using Taguchi’s orthogonal arrays - a subset of combinations is selected that provides sufficient information about the main effects and interactions and reduces the number of test cases while achieving proper coverage [13, 14]. The considered Taguchi array is presented in Table. 6.3.

Table 6.3: Taguchi array for the considered problem

Nr.	F1	F2	F3	F4	Nr.	F1	F2	F3	F4	Nr.	F1	F2	F3	F4	Nr.	F1	F2	F3	F4	Nr.	F1	F2	F3	F4
1	1	1	2	1	6	2	1	2	3	11	3	1	1	2	16	4	1	2	2	21	5	1	1	1
2	1	2	2	2	7	2	2	3	1	12	3	2	4	1	17	4	2	2	3	22	5	2	1	2
3	1	1	1	3	8	2	3	2	2	13	3	3	1	2	18	4	3	1	1	23	5	3	2	1
4	1	4	4	1	9	2	4	1	1	14	3	4	1	3	19	4	4	2	2	24	5	4	1	2
5	1	5	1	1	10	2	5	1	2	15	3	5	2	1	20	4	5	3	1	25	5	5	1	3

7. Synthetic data folder structure

The data folders are presented in Fig. 7.1, where:

- images, indicates the images generated by the physics-based camera sensor, available in Simcenter Prescan.
- labels indicate the ground truth data.
- pbLidar indicates that the data has been generated using physics-based LiDAR sensor model available in Simcenter Prescan.
- pbRadar indicate that the data has been generated using physics-based radar sensor models available in Simcenter Prescan.
- pointCloud, indicates the ideal point cloud generated by the ideal LiDAR sensor, available in Simcenter Prescan.

Name	Date modified	Type	Size
depthMap	5/30/2025 4:25 PM	File folder	
images	5/30/2025 4:25 PM	File folder	
labels	5/30/2025 4:25 PM	File folder	
pbLidar	5/30/2025 4:25 PM	File folder	
pbRadar	5/30/2025 4:25 PM	File folder	
pointCloud	5/30/2025 4:25 PM	File folder	
labelDataCombined	5/30/2025 4:25 PM	Comma Separate...	1,059 KB
prescanParameters	5/30/2025 4:25 PM	JSON Source File	3 KB
prescanParameters	5/25/2025 12:46 PM	MATLAB Data	223 KB
video	5/30/2025 4:25 PM	MP4 Video File (V...	29,432 KB
video_DEP	5/30/2025 4:25 PM	MP4 Video File (V...	38,965 KB
video_PCL	5/30/2025 4:26 PM	AVI Video File (VLC)	17,111 KB
video_PCS	5/30/2025 4:28 PM	AVI Video File (VLC)	32,343 KB
video_RSS	5/30/2025 4:28 PM	AVI Video File (VLC)	2,490 KB

Fig. 7.1 Data folder structure

8. References

1. Andreas Geiger, Philip Lenz and Raquel Urtasun - Are we ready for Autonomous Driving? The KITTI Vision Benchmark Suite, Conference on Computer Vision and Pattern Recognition (CVPR), 2012.
2. KITTI: The KITTI Vision Benchmark Suite, <https://www.cvlibs.net/datasets/kitti/>, accessed March 19, 2025.
3. SIEMENS. Simcenter Prescan. <https://plm.sw.siemens.com/en-US/simcenter/autonomous-vehicle-solutions/prescan/>(accessed November 26, 2024).
4. Pharr M, Jakob W, Humphreys G. Physically Based Rendering. From Theory to Implementation. Third Edition: Morgan Kaufmann Publishers Inc; 2016.
5. Basler camera: <https://www.baslerweb.com/en/shop/a2a1920-51gcpro/>, accessed March 19, 2025.
6. Ouster OS2: High-Precision Long-range Lidar for Autonomous Systems, <https://ouster.com/products/hardware/os2-lidar-sensor>, accessed March 19, 2025.
7. Christian Waldschmidt, Juergen Hasch and Wolfgang Menzel - Automotive Radar — From First Efforts to Future Systems. IEEE Journal of Microwaves. 1. 135-148, 2021.
8. Radar tutorial: <https://www.radartutorial.eu/07.waves/wa13.en.html>, accessed March 19, 2025.
9. Recommendation 838 – Specific attenuation model for rain for use in prediction methods, https://www.itu.int/dms_pubrec/itu-r/rec/p/R-REC-P.838-0-199203-S!!PDF-E.pdf, accessed March 19, 2025.
10. Recommendation 840 - Attenuation due to clouds and fog, <https://www.itu.int/rec/R-REC-P.840/en>, accessed March 19, 2025.
11. Recommendation ITU-R P.676-9 – Attenuation by atmospheric gases, https://www.itu.int/dms_pubrec/itu-r/rec/p/R-REC-P.676-9-201202-S!!PDF-E.pdf, accessed March 19, 2025.
12. Sun Earth Tools: Calculation of sun's position in the sky for each location on the earth at any time of day, https://www.sunearthtools.com/dp/tools/pos_sun.php?lang=en, accessed March 19, 2025.
13. R. N. Kacker, D. R. Kuhn Y.Lei D. E. Simos, "Factorials Experiments, Covering Arrays, and Combinatorial Testing", Mathematics in Computer Science, 2021, <https://doi.org/10.1007/s11786-021-00502-7>.
14. A. Forrai, K.K. Unni, V. Neelgundmath, H. Hotait, H. Abdolhay and I. Barosan - Safety assurance of AI-enabled sensing and perception subsystem used in autonomous vehicles, Springer, 2025 (to be published).